

# MODELING AND ANALYSIS OF THYRISTOR AND DIODE REVERSE RECOVERY IN RAILGUN PULSED POWER CIRCUITS\*

**J. Bernardes**

*Naval Surface Warfare Center, Dahlgren Division  
Dahlgren, VA 22448*

**S. Swindler**

*Naval Surface Warfare Center, Carderock Division  
Philadelphia, PA 19112*

## Abstract

As pulsed-power systems used to drive EM launchers evolve from laboratory to operational environments, high-power solid-state devices are emerging as the leading switch technology for these systems. These devices, specifically high-power thyristors and diodes, offer the advantages of improved energy efficiency, reduced volume, and reduced auxiliaries over spark-gaps and ignitrons. Proper application of these devices requires understanding of their behavior both during forward conduction and during reverse recovery.

The semiconductor device models available in most circuit simulation software packages do not accurately characterize large power thyristors and diodes for thermal management and snubber design. A semiconductor-device model is presented that captures device reverse-recovery and on-state conduction behavior utilizing a time-varying resistance that depends on the solid-state device properties and operating circuit parameters. The information needed to construct this model can be extracted from the device datasheet or obtained from the manufacturer.

This circuit model is used to analyze pulsed-power circuits typically used to drive railguns. Of key interest in these simulations are the voltage transients and energy losses in the solid-state devices during the reverse-recovery process. This behavior is analyzed for different circuit element values and device parameters such as peak reverse current, and reverse recovery charge.

## I. INTRODUCTION

In capacitor-based pulsed power circuits used to drive railguns, the large energy store is normally divided into modules. Groups of these modules are sequentially switched into the launcher to tailor pulse shape and amplitude. Figure 1 shows the two basic types of module circuits, with the main difference being the location of the crowbar diode.

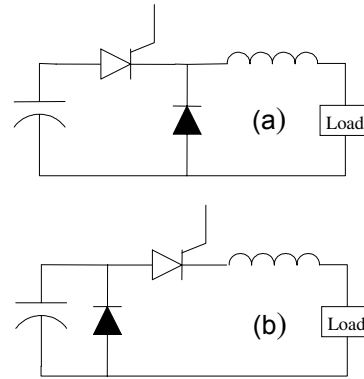


**Figure 1.** Two common circuit configuration for railgun capacitor-based pulsed power modules.

This type of circuit produces a current pulse with a sinusoidal rise to peak current, followed by an exponential decay. The initial part of the pulse is the result of the charged capacitor discharging through an underdamped, series, RLC circuit. At peak current, which corresponds to capacitor zero voltage, all the energy is stored in the system inductances, and, under ideal conditions, the crowbar diode prevents voltage reversal across the capacitor. This leads to current decaying exponentially as the inductor discharges through the diode and the load. Each of the two module-circuit topologies has advantages and disadvantages that impact the switch design. In Figure 1(a), where the diode is directly across the capacitor, the switch must conduct during the entire current pulse. In Figure 1(b), where the diode is on the load side of the switch, the switch only conducts during the current rise, greatly reducing switch losses and heating. However, because of unavoidable stray inductance between the capacitor and the diode, and because of thyristor reverse recovery behavior; there is a possibility for the generation of significant and potentially damaging transient voltages across the thyristor. Proper understanding of the thyristor reverse recovery behavior and the resultant voltage transients is essential when applying this circuit configuration.

This paper describes a circuit model for the thyristor that was specifically developed to facilitate transient

\* Work supported in part by NAVSEA PMS-405 and Office of Naval Research

## Report Documentation Page

*Form Approved*  
*OMB No. 0704-0188*

Public reporting burden for the collection of information is estimated to average 1 hour per response, including the time for reviewing instructions, searching existing data sources, gathering and maintaining the data needed, and completing and reviewing the collection of information. Send comments regarding this burden estimate or any other aspect of this collection of information, including suggestions for reducing this burden, to Washington Headquarters Services, Directorate for Information Operations and Reports, 1215 Jefferson Davis Highway, Suite 1204, Arlington VA 22202-4302. Respondents should be aware that notwithstanding any other provision of law, no person shall be subject to a penalty for failing to comply with a collection of information if it does not display a currently valid OMB control number.

1. REPORT DATE <b>JUN 2005</b>	2. REPORT TYPE <b>N/A</b>	3. DATES COVERED <b>-</b>			
4. TITLE AND SUBTITLE <b>Modeling And Analysis Of Thyristor And Diode Reverse Recovery In Railgun Pulsed Power Circuits</b>		5a. CONTRACT NUMBER			
		5b. GRANT NUMBER			
		5c. PROGRAM ELEMENT NUMBER			
6. AUTHOR(S)		5d. PROJECT NUMBER			
		5e. TASK NUMBER			
		5f. WORK UNIT NUMBER			
7. PERFORMING ORGANIZATION NAME(S) AND ADDRESS(ES) <b>Sandia National Laboratories, P.O. Box 5800, MS-1182, Albuquerque, NM 87185</b>		8. PERFORMING ORGANIZATION REPORT NUMBER			
9. SPONSORING/MONITORING AGENCY NAME(S) AND ADDRESS(ES)		10. SPONSOR/MONITOR'S ACRONYM(S)			
		11. SPONSOR/MONITOR'S REPORT NUMBER(S)			
12. DISTRIBUTION/AVAILABILITY STATEMENT <b>Approved for public release, distribution unlimited</b>					
13. SUPPLEMENTARY NOTES <b>See also ADM002371. 2013 IEEE Pulsed Power Conference, Digest of Technical Papers 1976-2013, and Abstracts of the 2013 IEEE International Conference on Plasma Science. IEEE International Pulsed Power Conference (19th). Held in San Francisco, CA on 16-21 June 2013., The original document contains color images.</b>					
14. ABSTRACT <b>As pulsed-power systems used to drive EM launchers evolve from laboratory to operational environments, highpower solid-state devices are emerging as the leading switch technology for these systems. These devices, specifically high-power thyristors and diodes, offer the advantages of improved energy efficiency, reduced volume, and reduced auxiliaries over spark-gaps and ignitrons. Proper application of these devices requires understanding of their behavior both during forward conduction and during reverse recovery.</b>					
15. SUBJECT TERMS					
16. SECURITY CLASSIFICATION OF:			17. LIMITATION OF ABSTRACT	18. NUMBER OF PAGES	19a. NAME OF RESPONSIBLE PERSON
a. REPORT <b>unclassified</b>	b. ABSTRACT <b>unclassified</b>	c. THIS PAGE <b>unclassified</b>	<b>SAR</b>	<b>4</b>	

behavior analysis of the capacitor module circuit during thyristor reverse recovery. This model can, however, also be adapted to any series RLC circuit containing a solid-state rectifier that experiences reverse conduction.

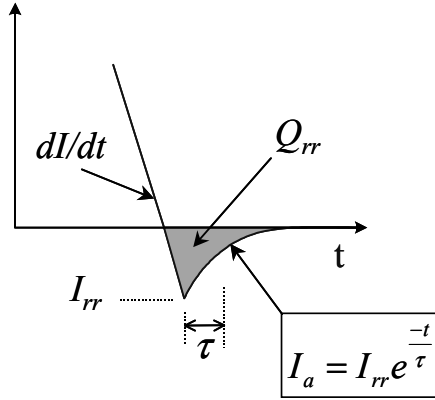


Figure 2. Rectifier approximate reverse-current behavior.

## II. RECTIFIER REVERSE RECOVERY

Solid-state rectifier devices such as thyristors and diodes conduct in the reverse direction to some degree during commutation. As the current passes through zero, the device continues to conduct due to excess minority carriers remaining in the device. These carriers require a certain amount of time to be removed by reverse current flow and by recombination with opposite charge carriers. This reverse-conduction behavior, known as reverse recovery and illustrated in Figure 2, is a function of device properties and the current derivative ( $dI/dt$ ) at the current zero crossing.

The reverse current can be approximated by a waveform with constant slope from zero to peak reverse current, followed by an exponential decay, with a time constant,  $\tau$ , derived from the specific device properties [1]. Two  $dI/dt$ -dependent parameters, peak reverse current,  $I_{rr}$ , and reverse charge,  $Q_{rr}$ , define the device reverse recovery behavior. These parameters are obtained from the device data sheet.  $Q_{rr}$  equals the integral of the reverse current, or, graphically – as shown in Figure 2, the area under the reverse current waveform. By integrating the reverse current, the following expression for  $Q_{rr}$  can be obtained in terms of the various waveform parameters.

$$Q_{rr} = \frac{I_{rr}^2}{2 \frac{dI}{dt}} + I_{rr} \tau \quad (1)$$

Solving the above equation for  $\tau$  yields the following:

$$\tau = \frac{Q_{rr}}{I_{rr}} - \frac{I_{rr}}{2 \frac{dI}{dt}} \quad (2)$$

$\tau$  gives a measure of how quickly the reverse current decays back to zero, and is a function of the device

properties,  $Q_{rr}$  and  $I_{rr}$ . A smaller  $\tau$  leads to a larger decaying-current derivative, and this results in higher voltage transients due to the presence of inductance in the circuit.

## III. RECTIFIER RECOVERY MODEL

A number of papers have presented thyristor and diode device models that capture some of the devices' complex behavior [2]-[8], but these were not convenient to use in railgun simulations. Semiconductor physics-based models [2] were not easily implemented in simulation packages and required knowledge of parameters not readily available to device users. Some papers did not address reverse recovery adequately [3]-[5]. Others did address reverse recovery but were considered overly complex and difficult to implement [6]-[8].

A recovery model for high-power silicon rectifiers was developed to produce the desired reverse-recovery behavior in a transient circuit model. This model consists of a time-varying resistance that increases at the appropriate rate to force the recovery current to decay in the time scale dictated by the device parameters and the zero-crossing  $dI/dt$ . This model is derived specifically for the thyristor used as a switch in a railgun pulsed power module with the crowbar diode forward of the switch. Similar procedures can be used to derive comparable expressions for the crowbar diode in this circuit, or for devices in other circuit configurations.

During forward conduction and up to peak reverse current, the rectifier can be modeled as a constant resistance, as a resistance in series with a dc threshold voltage, or using a more complex voltage drop model provided by the manufacturer. After  $I_{rr}$  is reached, an expression is derived for the rectifier effective resistance. This is done by first writing the following voltage loop equation for the circuit in Figure 3, which represents the module circuit during reverse recovery.

$$V_0 - \frac{1}{C} \int I_a dt = I_a R + L \frac{dI_a}{dt} + I_a R_{SCR} - V_d \quad (3)$$

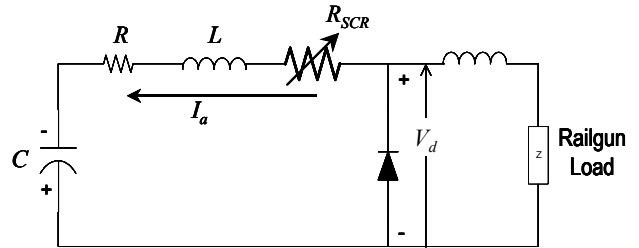


Figure 3. Module circuit used to derive the reverse recovery resistance.

$C$  is the energy storage capacitor, and  $V_0$  is the negative voltage on the capacitor resulting from the reverse conduction in the interval prior to  $I_{rr}$  being reached.  $L$  is

the stray inductance between the switch and the capacitor, and  $I_a$  is the reverse current from  $I_r$  forward. The recovery current can be modeled as a decaying exponential of the form shown below [1].

$$I_a = I_{rr} e^{-\frac{t}{\tau}} \quad (4)$$

Substituting this expression into (3), solving the derivative and integral, and rearranging terms, yields the following equation for the rectifier recovery resistance.

$$R_{SCR} = \frac{(V_0 + V_d)}{I_{rr}} e^{\frac{t}{\tau}} + \frac{\tau}{C} - R + \frac{L}{\tau} \quad (5)$$

This resistance has the form of an increasing exponential with a time constant,  $\tau$ .

#### IV. CIRCUIT MODEL ANALYSIS

The rectifier resistor model was evaluated in a test circuit using Microcap circuit analysis software. The selected circuit is that of a capacitor-store railgun module with the diode on the load side of the switch. Since, in this particular circuit, the diode does not experience reverse recovery, only the thyristor switch was modeled using the variable resistor. This circuit, shown in Figure 4, models a thyristor switch composed of two series ABB 5STP-26N6500 devices. Parallel resistor R23 represents static sharing resistors.

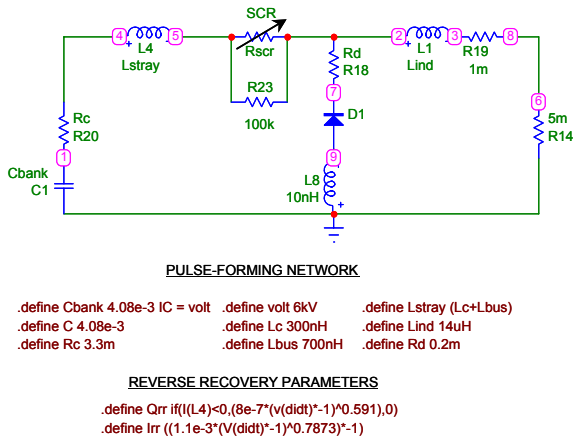


**Figure 4.** Microcap circuit model used to simulate Thyristor (SCR) reverse recovery behavior.

To facilitate running different parametric cases that change the rectifier zero-crossing  $dI/dt$ , expressions are generated for  $I_r$  and  $Q_r$  as a function of  $dI/dt$ . This is done through curve fitting data points obtained from the

device data sheet. This also allows easy extrapolation of these curves to higher  $dI/dt$  outside of the data specified, which is normally required when these devices are used in railgun pulsed power applications. As shown in Figure 5, a power-type curve fit achieves a good match to the data. In order to automate the process for different circuit conditions, the circuit model captures several parameters during the simulation. The first is the zero-crossing  $dI/dt$ , from which  $I_r$  and  $Q_r$  are calculated. This is followed capturing the time when the reverse current reaches  $I_r$ . These parameters are then used to calculate the rectifier recovery resistance in equation (5).

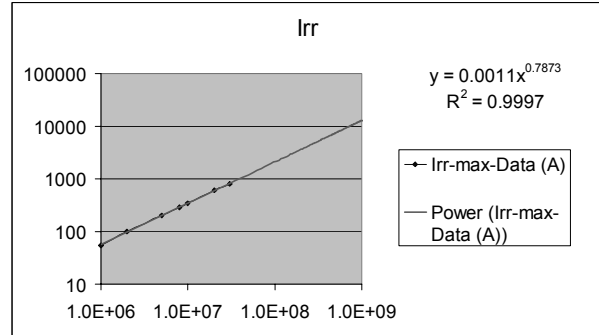


**Figure 5.** Curve fit to  $I_{rr}$  for ABB 5STP-26N6500 thyristor.

Figure 6 shows a set of waveforms generated by this circuit simulation. Figure 6(a) shows the thyristor and diode currents, the sum of which constitutes the sinusoidally rising, exponentially decaying load current. Note the reverse thyristor current with the characteristic initial constant  $dI/dt$  followed by the exponential decay to zero. As a check, integrating the reverse recovery current gives the recovery charge,  $Q_r$ , and this value should match the initially selected  $Q_r$ . Figure 6(b) shows the capacitor voltage and the thyristor voltage. Capacitor-voltage zero crossing coincides with thyristor peak current. The fall time of the thyristor current determines the degree of reverse voltage on the capacitor. The thyristor reverse voltage is in effect a pulse, due to the “snap back” of the recovery current, superimposed on the capacitor reverse voltage. Ultimately, the main functions of this type of simulation are: (1) to determine the reverse voltage on the thyristor to insure that rated reverse voltage magnitude is not exceeded; (2) if reverse-voltage mitigation is necessary, determine the value and impact of adding snubber components, and (3) determine the losses in the rectifier during the reverse recovery period.

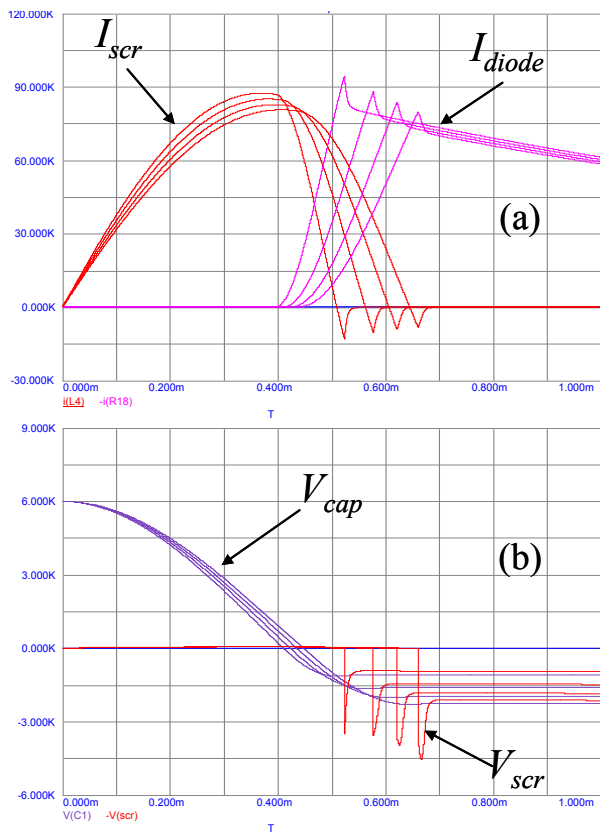


**Figure 6.** Sample waveforms showing thyristor reverse recovery, and the impact of varying stray inductance between capacitor and thyristor from 1 to 4  $\mu\text{H}$  in steps of 1  $\mu\text{H}$ .

Figure 6 shows another feature of this self-contained simulation approach, the stepping of component values in order to analyze trends. Figure 6 shows the impact of varying the stray inductance between the capacitor and the thyristor. Thyristor and diode currents along with capacitor and thyristor voltages are displayed for stray inductance values of 1, 2, 3, and 4 mH. This inductance is controlled by the geometry of the buswork, and is therefore driven by component layout. Increasing inductance results in longer fall times in thyristor current, and consequently lower  $dI/dt$ . This leads to lower  $I_{rr}$  and  $Q_{rr}$  values, higher capacitor reverse voltages, and, not necessarily intuitive, larger transient voltage pulsed on the thyristor voltage. Overall this example analysis indicates that it is advantageous to reduce this stray inductance.

## V. SUMMARY

A rectifier circuit model was developed that includes reverse recovery behavior. This model was implemented and demonstrated for a commercial high-power thyristor in a typical railgun pulsed-power circuit. The two main advantages of this modeling approach are: (1) the ability model both forward conduction and reverse recovery in a

single simulation run, and (2) the ability to quickly perform parametric analysis. This simulation approach is a tool for designing circuits where transients from the reverse recovery of solid-state rectifiers are a concern.

## VI. REFERENCES

- [1] J. Waldmeyer, B. Backlund, "Design of RC Snubbers for Phase Control Applications," ABB Document 5SYA 2020-01, Feb. 2001.
- [2] P. Lauritzen, C. Ma, "A simple diode model with reverse recovery," IEEE Transactions on Power Electronics, Apr. 1991.
- [3] S. Taib, L. Hulley, Z. Wu, W. Shepherd, "Thyristor switch model for power electronic circuit simulation in modified SPICE 2," IEEE Transactions on Power Electronics, Jul. 1992.
- [4] Y. Liang, V. Gosbell, "A versatile switch model for power electronics SPICE2 simulations", IEEE Transactions on Industrial Electronics, Volume 36, Issue 1, Feb. 1989.
- [5] P. McEwan, "Modelling of thyristors using manufacturers data," IEE Colloquium on Power Electronics and Computer Aided Engineering, Jan. 1994
- [6] Z. Gang, C. Xiangxun, Z. Jianchao, W. Chengqi, "A Macro-Model of SCR for Transient Analysis in Power Electronic System," POWERCON '98. Aug. 1998.
- [7] N. Losic, "Modeling of Thyristor Circuits in Computer-Aided Analysis and Design," APEC '88. Feb. 1988.
- [8] F. Gracia, F. Arizti, F. Aranceta, "A nonideal macromodel of thyristor for transient analysis in power electronic systems," IEEE Transactions on Industrial Electronics, Dec. 1990.